APPENDICES

APPENDIX I

Catalyst and bed characteristics

A prereduced and stabilized supported cobalt catalyst, Co-0164 T 1/8" from Engelhard de Meern B.V., was used in all the experimental runs. The catalyst particles were shaped as cylindrical pellets (diameter = 3.2 mm, length = 3.7 mm). The composition of the catalyst, specified by the supplier, was:

cobalt	5 %
cobalt oxide	26 %
silica, amorphous	50 %
alumina	4 %
graphite, synthetic	3 %

The total cobalt content of the catalyst was 23.2 % measured by atomic absorption.

Measurements of the internal surface area by the BET method, particle and solid density and pore volume and pore size distribution by mercury porosimetry and nitrogen sorption were performed at the Laboratory of Industrial Chemistry, NTH-Norwegian Institute of Technology, Trondheim.

Table AI-1 shows some characteristic data from the catalyst particle measurements and from the packed bed of particles. The bulk density of the catalyst bed was calculated from the reactor bed volume and catalyst weight. The value found was somewhat higher than the value denoted by the supplier. Care was taken to get an uniform and reproducible packing of the bed and the variation of catalyst mass between different loadings was less than 0.5 %.

Table AI–1. Catalyst and packed bed characteristics.

Bed volume, V_R (m^3)	0.736×10^{-3}
Catalyst mass, W (kg)	0.652
Catalyst bulk density, ρ_b (kg/m^3)	0.89×10^3
Catalyst particle density, ρ_p (kg/m^3)	1.59×10^3
Catalyst solid density, ρ_s (kg/m^3)	3.08×10^3
Catalyst pore volume, V_g (m^3/kg)	0.306×10^{-3}
Catalyst internal surface area, S_g (m^2/kg)	72.0×10^3
Void fraction of packed bed, $\varepsilon_0 = 1-(\rho_b/\rho_p)$	0.44
Void fraction of catalyst particle, ε_p	0.485
Catalyst particle equivalent spherical diameter, $d_p = 6(V_p/S_x)$ (m)	3.3×10^{-3}

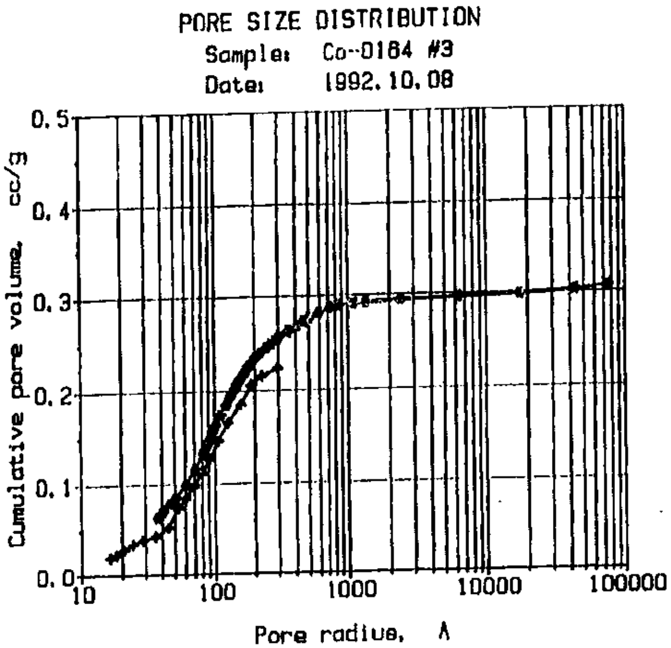
PORE SIZE DISTRIBUTION
Sample: Co-0164 #3
Date: 1992.10.08
Cumulative pore volume, cc/g
0.0
0.1
0.2
0.3
0.4
0.5
10
100
1000
10000
100000
Pore radius, Å

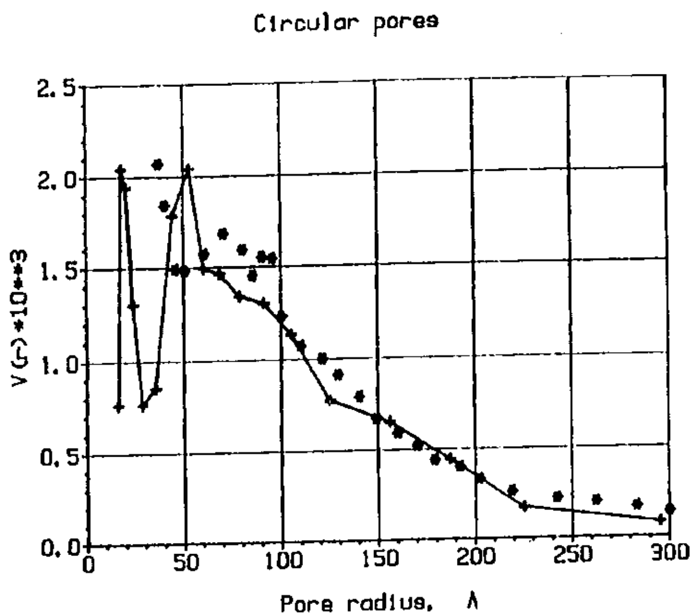
Circular pores
V(r)*10**3
0.0
0.5
1.0
1.5
2.0
2.5
0
50
100
150
200
250
300
Pore radius, Å

APPENDIX II

GC-analysis

A HP 5890A gas chromatograph equipped with a flame ionization detector (FID) and a thermal conductivity detector (TCD) was used for the analysis of gas composition. Helium (Norsk Hydro, 99.995 %) was used as carrier gas for both detectors. The carrier gas was passed through a gas purifier (Supelco High Capacity Gas Purifier) and an indicating purifier (OMI-1) for the removal of oxygen and water prior to entering the GC. Parameters for the GC-analysis are shown in table AII-1 and examples of chromatograms are shown in figures AII-1 and AII-2.

Table AII-1. GC-parameters

Detector	TCD	FID
Column	Carbosieve S-II 1/8" x 10'	J&W DB-1 5μm 0.53mm x 30m
Temp. sample valve (°C)	250	250
Temp. injector (°C)	250	250
Temp. detector (°C)	200	250
Temp. program		
Initial temp. (°C)	45	0
Initial time (min)	5	1
Rate (°C/min)	10	10
Final temp (°C)	225	220
Final time (min)	10	20
Gas flow (ml/min)		
Carrier gas	30	15
Reference gas	45	
Make-up gas		15
H_2		30
Air		340

The TCD was calibrated for the quantification of CO, CO_2 and CH_4 using a gas mixture of known comopsition with nitrogen as internal standard. Assuming a constant concentration of nitrogen, equal to the inlet concentration, through the reactor this method reports concentrations, C_i, in the same units as C_{N_2}. If temperature or pressure varies through the reactor the concentrations are reported at inlet temperature and pressure. Hydrogen was detected by this analytical configuration but the responce was very weak and the responce factor was strongly dependent on amount, using helium as carrier gas, making quantifications very inaccurate. Hydrogen concentrations are therefore not reported. Responce factors for the other componenets were insignificant dependent on amount.

Hydrocarbon distribution was determined by the FID detector. Methane was used as internal standard with C_{CH_4} arbitrarily set to 1. Molar responce factors of the FID for C_1–C_4 were obtained from a calibration performed by Rune Lødeng at SINTEF, Trondheim, on a HP 5890 GC with a wide bore capillary column similar to the one used in this study. For the higher hydrocarbons the responce factor of C_4 was used with a correction for the difference in number of carbon atoms. The factors used for the FID analyses were recalculated to a weight fraction basis and compared with the factors reported by Dietz (Dietz, 1967) and the agreement was found to be good.

Alcohols were not detected in the product and the amount of alkenes and isoalkanes were low compared with n-alkanes. The amounts of all products having the same number of carbon atoms were therefore added together and reported as a C_n-fraction. An example of an approximate weight composition of all hydrocarbon products up to C_{22} are shown in figure AII-3.

Calculations of hydrocarbon concetrations in the same units as C_{N_2} can be done using equation AII-1.

$$C_n = X_n \cdot C_{CH_4} \qquad \text{(AII-1)}$$

Here C_n is the concentration of the hydrocarbon fraction with n carbon atoms, X_n is the molar ratio of hydrocarbons with n carbon atoms relative to CH_4 as determined by the FID analysis and C_{CH_4} is the concentration of methane as determined by the TCD analysis.

Calculation of carbon number distribution and selectivity

Selectivities are reported as normalized carbon selectivities defined by equation (AII–2).

$$S_n = n \cdot C_n / \sum n \cdot C_n \qquad \text{(AII–2)}$$

where S_n is the selectivity to products with n carbon atoms and C_n is the concentration.

The Schulz–Flory parameter α can be estimated from the relative molar ratios X_n of hydrocarbons by a plot of $\ln X_n$ versus n in accordance with the Schulz–Flory equation AII–3.

$$\ln X_n = n \cdot \ln\alpha - \ln\alpha \qquad \text{(AII–3)}$$

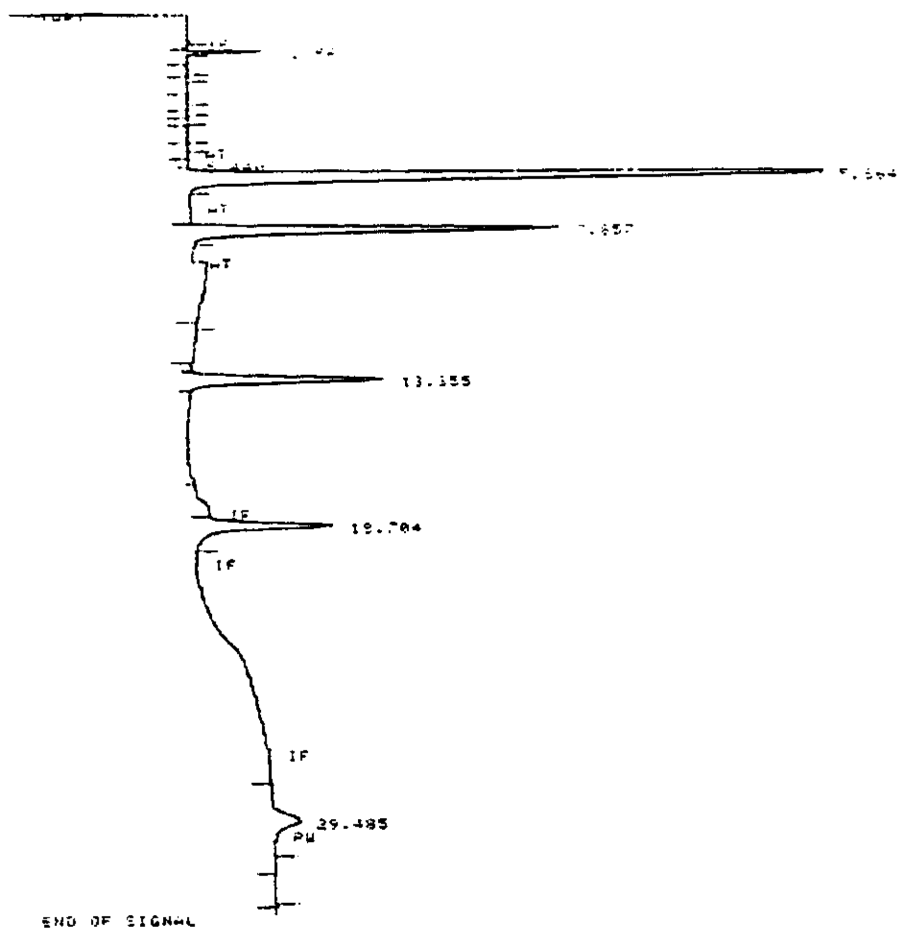

END OF SIGNAL

Storing report to H:03EED8CA.RPA
ILLEGAL EXTENSION NAME

RUN# 34 JAN 10, 1992 13:38:48

ISTD%-AREA

RT	TYPE	AREA	WIDTH	HEIGHT	CAL#	AMOUNT	NAME
1.356	BB	2606	.062	698	1	13.930	H2
5.664	PB	6529139	.284	382697	2*		N2
7.857	BB	402003	.243	27563	3	5.972	CO
13.355	PP	26838	.249	1800	4	.481	CH4
18.704	BB	19224	.254	1198	5	.198	CO2
29.485	PB	4558	.559	255	6	.107	C2H6

Figure AII–1. Example of a TCD chromatogram.

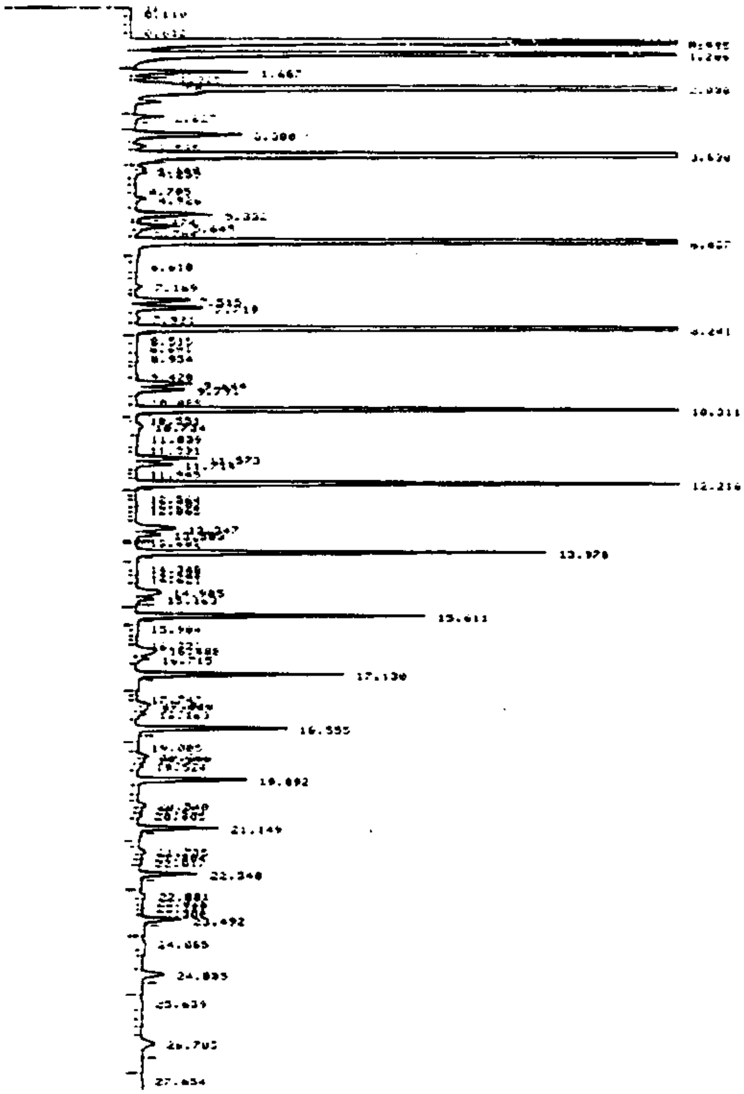

Figure AII-2. Example of a FID chromatogram.

NORM-AREA

RT	TYPE	AREA	WIDTH	HEIGHT	CAL#	AMOUNT	NAME
.639	PV	5363216	.056	1495206	1	16.147	C1
.725	VB	1955039	.046	773456	2	5.652	C2
1.206	PB	3513672	.054	1060146	3	11.669	C3
1.667	BV	158049	.066	47684		.540	
1.825	VP	33816	.042	12201		.114	
2.086	PB	3485088	.052	706201	4	11.742	C4
2.627	BB	47701	.064	12227		.161	
3.302	BP	257605	.095	45290		.672	
3.595	PP	19711	.071	4611		.067	
3.630	PB	3221070	.060	571254	5	10.699	C5
4.146	PV	11302	.053	2454		.036	
4.259	VP	19631	.062	977		.064	
4.926	PV	21555	.081	4444		.073	
5.032	VV	175194	.090	32741		.592	
5.474	VV	8514	.052	2294		.029	
5.645	VV	99957	.049	19610		.335	
5.794	VP	11096	.073	2522		.037	
6.057	PB	1591526	.075	353717	6	5.725	C6
7.497	PV	11013	.071	2575		.037	
7.515	PV	116962	.066	22746		.395	
7.719	VV	144630	.066	29011		.469	
7.961	VP	11218	.113	1651		.038	
8.241	PB	1945566	.077	423665	7	6.563	C7
9.644	VV	130460	.094	23143		.441	
9.791	VP	103075	.085	20261		.349	
10.311	VB	1426507	.074	322917	8R	4.027	C8
10.734	VV	24365	.166	2450		.083	
11.573	VV	127607	.064	25390		.432	
11.714	VP	70219	.079	14870		.230	
12.218	VB	1039369	.073	237050	9	3.517	C9
13.347	PV	112785	.114	16545		.382	
13.503	VB	49080	.060	10286		.166	
13.970	BB	759519	.073	172705	10	2.570	C10
14.985	PV	93253	.154	10078		.316	
15.163	VB	33293	.070	7104		.113	
15.611	PB	532913	.073	121011	11	1.803	C11
16.400	VV	61916	.172	7945		.277	
16.715	VP	23170	.070	4951		.078	
17.130	PB	383177	.076	86772	12	1.297	C12
17.918	VV	30343	.092	5587		.103	
17.997	VV	28050	.112	4307		.098	
18.163	VP	16309	.077	3523		.055	
18.555	PB	278540	.074	62584	13	.943	C13
19.266	VV	24918	.096	4206		.084	
19.359	VV	20203	.113	2985		.068	
19.524	VP	11162	.077	2419		.038	
19.692	PV	209211	.076	45763	14	.708	C14
20.540	VV	20858	.107	3253		.071	
20.651	VV	14599	.116	2183		.049	
20.805	VP	7952	.077	1721		.027	
21.149	PB	147404	.075	32856	15	.499	C15
21.735	PV	15836	.108	2442		.054	
21.864	VV	9756	.113	1435		.033	
22.017	VP	5167	.076	1138		.017	
22.340	PB	112674	.078	24058	16	.381	C16
22.881	PV	12676	.111	1904		.043	
23.026	VV	6813	.112	1013		.023	
23.492	VB	64509	.088	15984	17	.206	C17
24.065	BV	12130	.157	1205		.041	
24.665	PB	64034	.116	9105	18	.217	C18
25.639	BV	11992	.206	971		.041	
26.703	VB	51534	.157	5461	19	.174	C19
27.654	BV	6346	.275	384		.021	
29.119	VB	44623	.229	3251	20	.151	C20
30.365	PV	5798	.305	251		.020	
32.353	PV	32421	.296	3025	21	.110	C21
36.736	PP	23853	.309	1021	22	.081	C22

Figure AII–3. Example of an approximate weight fraction composition of hydrocarbon products from C_1 to C_{22}.

Experimental data for run 1

Experimental conditions:

Oil temperature:	497 K
Inlet temperature:	498 K
Inlet pressure:	1.0 MPa
GHSV:	540 Nl_{H_2+CO} / kg catalyst · h
Inlet N_2 conc.:	186 mol / m^3
Inlet H_2 conc.:	38.2 mol / m^3
Inlet CO conc.:	17.4 mol / m^3

Analytical results:

TOS (h)	Axial pos. (m)	C_{CO} (mol/m^3)	C_{CO_2} (mol/m^3)	C_{CH_4} (mol/m^3)	C_2/C_3– ratio	α
1.00	0.15	16.39	0.03	0.12	0.99	0.70
2.50	0.30	15.55	0.11	0.30	0.91	0.68
4.00	0.45	14.72	0.14	0.47	0.94	0.68
6.00	0.60	13.99	0.19	0.59	0.96	0.67
7.50	0.75	13.18	0.12	0.73	0.90	0.67
9.00	0.90	12.73	0.17	0.79	0.88	0.68
11.00	1.05	12.15	0.15	0.87	0.94	0.68
22.50	1.50	11.11	0.37	0.89	0.88	0.69

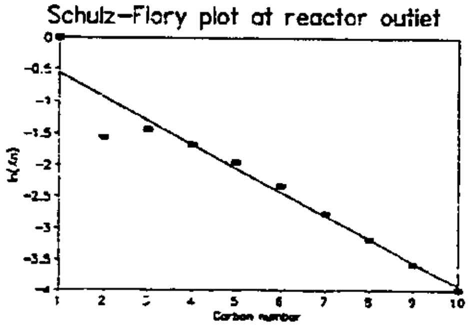

Experimental data for run 2

<u>Experimental conditions:</u>

Oil temperature:	499 K
Inlet temperature:	503 K
Inlet pressure:	1.0 MPa
GHSV:	400 Nl_{H_2+CO} / kg catalyst · h
Inlet N_2 conc.:	196.1 mol / m^3
Inlet H_2 conc.:	29.6 mol / m^3
Inlet CO conc.:	13.5 mol / m^3

<u>Analytical results:</u>

TOS (h)	Axial pos. (m)	C_{CO} (mol/m^3)	C_{CO_2} (mol/m^3)	C_{CH_4} (mol/m^3)	C_2/C_3-ratio	α
10.75	0.30	11.77	0.06	0.38	0.96	0.63
13.00	0.60	10.20	0.09	0.64	0.88	0.63
14.75	0.90	9.01	0.08	0.83	0.90	0.63
16.75	1.20	7.87	0.20	0.97	0.91	0.64
18.75	1.50	6.93	0.24	1.08	0.86	0.64
20.75	0.15	12.31	0.00	0.14	0.91	0.65
22.75	0.45	11.00	0.05	0.41	0.88	0.64
24.50	0.75	10.16	0.11	0.56	0.92	0.65
26.50	1.05	9.18	0.08	0.70	0.84	0.65
28.50	1.35	7.76	0.68	0.85	0.85	0.65

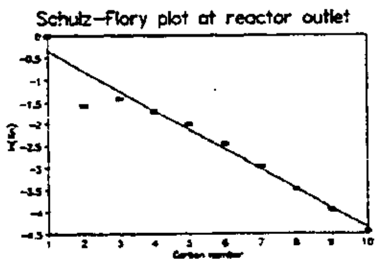

Experimental data for run 3

Experimental conditions:

Oil temperature:	499 K
Inlet temperature:	500 K
Inlet pressure:	1.0 MPa
GHSV:	670 Nl_{H_2+CO} / kg catalyst · h
Inlet N_2 conc.:	168.4 mol / m^3
Inlet H_2 conc.:	49.6 mol / m^3
Inlet CO conc.:	22.6 mol / m^3

Analytical results:

TOS (h)	Axial pos. (m)	C_{CO} (mol/m^3)	C_{CO_2} (mol/m^3)	C_{CH_4} (mol/m^3)	C_2/C_3-ratio	α
9.25	0.30	21.83	0.00	0.17	0.92	0.69
11.25	0.60	20.86	0.00	0.33	0.89	0.68
13.00	0.90	19.86	0.00	0.46	0.89	0.68
15.00	1.20	18.88	0.09	0.59	0.89	0.68
17.00	1.50	17.38	0.57	0.74	0.93	0.68
19.00	0.15	22.50	0.00	0.09	1.11	0.69
21.00	0.45	21.65	0.00	0.22	0.90	0.68
22.75	0.75	20.79	0.03	0.36	0.88	0.68
24.75	1.05	20.13	0.00	0.44	0.87	0.68
26.75	1.35	17.53	0.98	0.73	1.13	0.68

Schulz-Flory plot at reactor outlet

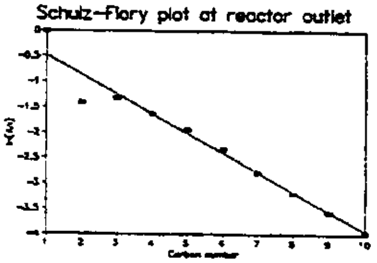

Example of a runaway progression

Figure AII–4 shows the progression of the centerline temperature profile after a step increase in the partial pressure of synthesis gas causing runaway.

Experimental conditions:

Temperature: 495 K

Total pressure: 1.0 MPa

N_2 flow: 20 Nl/min

The partial pressure of H_2/CO was increased from 0.23 MPa to 0.31 MPa.

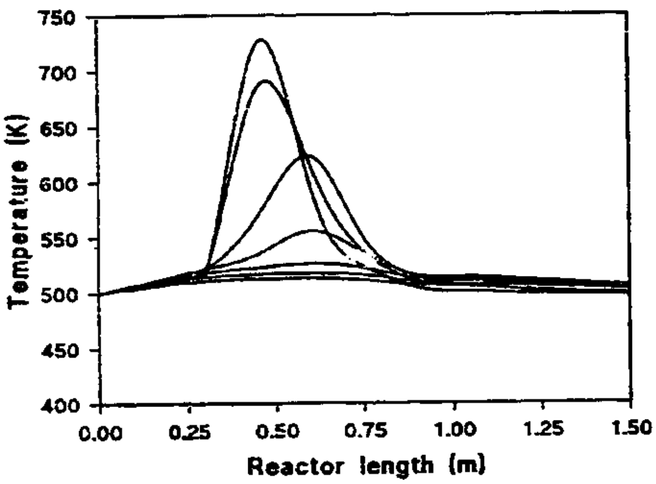

Figure AII–4. Centerline temperature profiles recorded at 1 min. intervals after a step change in partial pressure of synthesis gas, starting at steady state.

REFERENCES

Dietz, W.A., *J. Gas Chromatogr.*, 5(1967), 68.

APPENDIX III

Rate expressions for the Fischer-Tropsch kinetics

The stoichiometry and heat of reaction for the reactions considered in the kinetic model are shown in equation AIII-1 and AIII-2.

$$CO + (2+1/n)H_2 \rightarrow (1/n)C_nH_{2n+2} + H_2O, \quad \Delta H_R = -165 \text{ kJ} \tag{AIII-1}$$

$$CO + 3H_2 \rightarrow CH_4 + H_2O, \quad \Delta H_R = -215 \text{ kJ} \tag{AIII-2}$$

The rate of CO consumption and the rate of CH_4 formation are shown in equation AIII-3 and AIII-4.

$$-r_{CO} = \frac{(1 - \beta_{CO} t)\, A'_{CO}\, e^{-\frac{E_{CO}}{RT_0}\left(\frac{1-\theta}{\theta}\right)}\, P_{CO}\, P_{H_2}}{(1 + K_{CO}\, P_{CO})^2} \tag{AIII-3}$$

$$r_{CH_4} = \frac{(1 - \beta_{CH_4} t)\, A'_{CH_4}\, e^{-\frac{E_{CH_4}}{RT_0}\left(\frac{1-\theta}{\theta}\right)}\, P_{CO}^{1/2}\, P_{H_2}}{(1 + K_{CO}\, P_{CO})^2} \tag{AIII-4}$$

In expression AIII-3 and AIII-4 β is the rate of deactivation, t is time in hours, K_{CO} is the adsorption constant and P is partial pressure in MPa. For computational reasons the special form of the Arrhenius expression shown in the equations was chosen. A' is the modified preexponential factor related to the preexponential factor A through: $A' = A \exp(-E/RT_0)$ where T_0 is the inlet temperature, E the activation energy and θ is the dimensionless temperature defined as T/T_0.

The rate of formation of hydrocarbon product with n carbon atoms is related to the rate of C_3 formation by the Schulz-Flory distribution shown in equation AIII-5.

$$r_n = r_3\,\alpha^{n-3} \quad , \quad n \geq 3 \tag{AIII-5}$$

Rates of formation of products and r_{H_2} can be related to r_{CO} and r_{CH_4} by carbon (equation AIII-6) and hydrogen (equation AIII-7) balances.

$$r_{CO} + r_{CH_4} + 2r_2 + \sum_{n=3}^{\infty} n r_n = 0 \tag{AIII-6}$$

$$r_{H_2} + r_{H_2O} + 2r_{CH_4} + 3r_2 + \sum_{n=3}^{\infty} (n+1) r_n = 0 \tag{AIII-7}$$

Introducing the Schulz-Flory equation AIII-5, the C_2/C_3 ratio γ and $r_{H_2O} = -r_{CO}$ in these equations give:

$$r_{CO} + r_{CH_4} + 2\gamma r_3 + r_3 \sum_{n=3}^{\infty} n\alpha^{n-3} = 0 \tag{AIII-8}$$

$$r_{H_2} - r_{CO} + 2r_{CH_4} + 3\gamma r_3 + r_3 \sum_{n=3}^{\infty} (n+1)\alpha^{n-3} = 0 \tag{AIII-9}$$

The summations in AIII-8 and AIII-9 can be replaced by:

$$S_1 = \sum_{n=3}^{\infty} n\alpha^{n-3} = \frac{3-2\alpha}{(1-\alpha)^2} \tag{AIII-10}$$

$$S_2 = \sum_{n=3}^{\infty} (n+1)\alpha^{n-3} = \frac{4-3\alpha}{(1-\alpha)^2} \tag{AIII-11}$$

From the values of r_{CO} from equation AIII-3 and r_{CH_4} from equation AIII-4, the other rates can then be calculated.

$$r_3 = -\frac{r_{CO} + r_{CH_4}}{2\gamma + S_1} \qquad \text{(AIII-12)}$$

$$r_{H_2} = -[- r_{CO} + 2r_{CH_4} + r_3(3\gamma + S_2)] \qquad \text{(AIII-13)}$$

$$(-\Delta H)r_v = 215000 \cdot r_{CH_4} - 165000 \cdot (r_{CO} + r_{CH_4}) \qquad \text{(AIII-14)}$$

r_a can be calculated from equation AIII-5, $r_2 = \gamma r_3$ and $r_{H_2O} = -r_{CO}$.

APPENDIX IV

Radial porosity and velocity profiles

The radial porosity profile is approximated by:

$$e(r) = C_1 (1 + C_2 e^{\frac{2}{d_p} r}) \qquad \text{(AIV-1)}$$

where d_p is the particle diameter, r is radial coordinate and C_1 and C_2 are unknown constants.

The porosity is unity at the wall, and the average porosity across the tube must equal the porosity ε_0 determined from the density of the bed and the density of the particles. These requirements are expressed by equation AIV-2 and AIV-3.

$$\varepsilon(1) = 1 \qquad \text{(AIV-2)}$$

$$2\pi \int_0^R e(r) r\,dr = 2\pi \int_0^R \left[C_1 (1 + C_2 e^{\frac{2}{d_p} r}) \right] r\,dr = \pi R^2 e_0 \qquad \text{(AIV-3)}$$

This gives the following expressions for C_1 and C_2:

$$C_2 = \frac{1 - e_0}{\left(e_0 - \frac{d_p}{R} + \frac{1}{2} (\frac{d_p}{R})^2 \right) e^{\frac{2R}{d_p}} - \frac{1}{2} (\frac{d_p}{R})^2} \qquad \text{(AIV-4)}$$

$$C_1 = \frac{1}{1 + C_2 e^{\frac{2R}{d_p}}} \qquad \text{(AIV-5)}$$

Analytical expression for the evaluation of radial superficial flow profiles. From Vortmeyer and Schuster, 1983.

$$\frac{v}{v_0} = b\left[1 - \left(1 - nR'(1-r')\right)e^{aR'(1-r')}\right] \quad \text{(AIV-6)}$$

where r' is dimensionless radial coordinate and R' is defined as $R' = R/d_p$.

The constants a, b and n in equation AIV–6 are correlated to the mean velocity through the Reynolds number.

$$n = -1803 + 201.62(\ln Re_p + 4) - 3737(\ln Re_p + 4)^{1/2} + 5399(\ln Re_p + 4)^{1/3} \quad \text{(AIV-7)}$$

for $1 \le Re_p \le 1000$

$$a = \frac{4n}{4 - n} \quad \text{(AIV-8)}$$

$$b = \frac{R'^2}{2}\left[\frac{R'^2}{2} - \frac{(nR' - 1)(aR' - 1)}{a^2} + n\left(\frac{R'^2}{a} + \frac{2R'}{a^2} + \frac{2}{a^3}\right) - \frac{e^{aR'}}{a^2}\left(1 - nR' + \frac{2n}{a}\right)\right]^{-1} \quad \text{(AIV-9)}$$

Wall boundary conditions for the heat conduction model

Derivation of an overall heat transfer coefficient

The heat balance equations are:
heat balance reactor

$$0 = -v\rho_g C_{pg}\frac{\partial T}{\partial z} + \lambda_{ax}\frac{\partial^2 T}{\partial z^2} + \frac{1}{r}\frac{\partial}{\partial r}(r\lambda_r\frac{\partial T}{\partial r}) + \rho_b\frac{(1-\epsilon)}{(1-\epsilon_0)}(-\Delta H)r_v \qquad \text{(AIV-10)}$$

heat balance wall

$$\lambda_w\frac{1}{r}\frac{\partial}{\partial r}(r\frac{\partial T}{\partial r}) = 0 \qquad \text{(AIV-11)}$$

Boundary condition between packed bed and reactor wall

$$\lambda_r\frac{\partial T}{\partial r}\Big|_{r=R^-} = \lambda_w\frac{\partial T}{\partial r}\Big|_{r=R^+} \qquad \text{(AIV-12)}$$

Boundary condition at coolant side

$$-\lambda_w\frac{\partial T}{\partial r}\Big|_{r=R_0} = \alpha_c(T_{R_0}-T_c) \qquad \text{(AIV-13)}$$

The general solution of equation AIV-11 is

$$T = C_1\ln r + C_2 \qquad \text{(AIV-14)}$$

and

$$\frac{\partial T}{\partial r} = \frac{C_1}{r} \qquad \text{(AIV-15)}$$

A relation can be found between the wall temperatures at the bed side and the coolant side by use of equation AIV-14 at these locations, eliminating the constant C_2.

$$T_{R_o} = C_1 \ln(R_O/R) + T_R \qquad \text{(AIV-16)}$$

The constant C_1 is determined from equation AIV-13 by replacing T_{R_o} with equation AIV-16 and $\partial T/\partial r$ with equation AIV-15.

$$-C_1 = \frac{\alpha_c}{\lambda_w}\left[\frac{1}{R_O} + \frac{\alpha_C}{\lambda_w}\ln(\frac{R_O}{R})\right]^{-1}(T_R - T_c) \qquad \text{(AIV-17)}$$

Replacing the right hand side differential of equation AIV-12 with the expression given in equation AIV-15 and using the expression obtained in equation AIV-17 gives:

$$-\lambda_r \frac{\partial T}{\partial r}\bigg|_{r=R^-} = \frac{\alpha_c}{R}\left[\frac{1}{R_O} + \frac{\alpha_C}{\lambda_w}\ln(\frac{R_O}{R})\right]^{-1}(T_R - T_c) \qquad \text{(AIV-18)}$$

This shows that the heat balance reactor equation AIV-10 can be solved with the boundary condition

$$-\lambda_r \frac{\partial T}{\partial r}\bigg|_{r=R^-} = U_c(T_R - T_c) \qquad \text{(AIV-19)}$$

with an overall heat transfer coefficient U_c between the reactor inner wall and the coolant given by:

$$U_c = \frac{\alpha_c}{R}\left[\frac{1}{R_O} + \frac{\alpha_c}{\lambda_w}\ln(\frac{R_O}{R})\right]^{-1} \qquad \text{(AIV-20)}$$

Measured radial void fraction profiles. From Lerou and Froment, 1986.

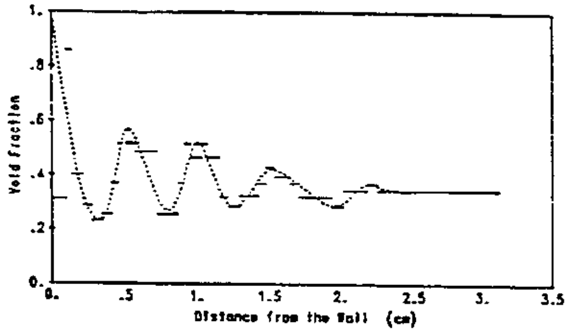

Measured radial void fraction profile of
a bed packed with small spheres.

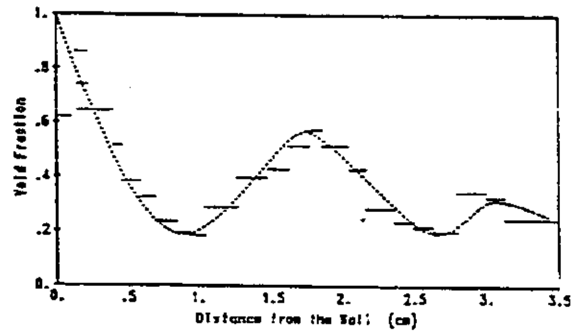

Measured radial void fraction profile of
a bed packed with large spheres.

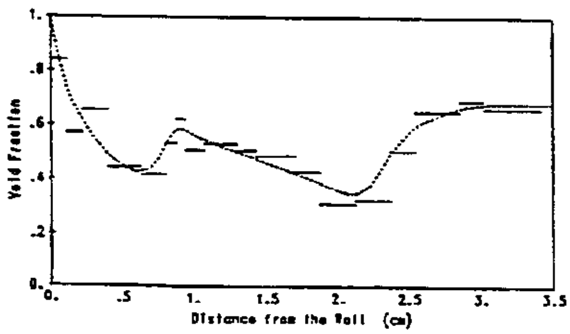

Measured radial fraction profile of a bed
packed with Raschig rings.

REFERENCES

Lerou, J.J., Froment, G.F., in "Chemical Reactor Design and Technology", ed.: de Lasa, H.I., NATO ASI series E, No. 110, Martinus Nijhoff Publishers, Dordrecht, The Netherlands, 1986, p. 729.

Vortmeyer, D., Schuster, J., Chem. Eng. Sci., 38(1983), 1691.

APPENDIX V

Calculation of differentials by cubic spline interpolation

Given a relationship y=f(x) between the dependent variable y and the independent variable x in the domain $x_1 \le x \le x_N$. The domain is divided into N−1 intervals by placing dividing points at x_i, i = 1,...,N. The values of y at the dividing points, y_i, are assumed to be known.

The function f(x) is approximated by cubic polynomals on the N−1 intervals.
For $x_i \le x \le x_{i+1}$:

$$y = y_i + b_i(x-x_i) + c_i(x-x_i)^2 + d_i(x-x_i)^3 \qquad \text{(AV-1)}$$

where b_i, c_i and d_i are unknown constants.

The constants are determined from the requirements of continuity of the function and its first and second derivatives at the dividing points.
By introducing $h_i = x_{i+1} - x_i$, $y'_i = dy/dx(x=x_i)$, $y''_i = d^2y/dx^2(x=x_i)$ and using the continuity of y", the continuity condition for y and y' can be obtained from equation AV−1 and its derivatives.

$$y_{i+1} = y_i + h_i y_i' + \frac{1}{3}h_i^2 y_i'' + \frac{1}{6}h_i^2 y_{i+1}'' \qquad \text{(AV-2)}$$

$$y_i' = y_{i-1}' + \frac{1}{2}h_i y_{i-1}'' + \frac{1}{2}h_i y_i'' \qquad \text{(AV-3)}$$

An expression for y'_i can be found from AV−2:

$$y_i' = -\frac{1}{h_i}y_i + \frac{1}{h_i}y_{i+1} - \frac{1}{3}h_i y_i'' - \frac{1}{6}h_i y_{i+1}'' \qquad \text{(AV-4)}$$

Eliminating y'_i and y'_{i-1} in equation AV–3 by use of equation AV–4 twice at x_{i-1} and x_i gives:

$$h_{i-1}y''_{i-1} + 2(h_{i-1}+h_i)y''_i + h_i y''_{i+1} = \frac{6}{h_{i-1}}y_{i-1} - \left(\frac{6}{h_{i-1}}+\frac{6}{h_i}\right)y_i + \frac{6}{h_i}y_{i+1} \qquad \text{(AV–5)}$$

$$for\ i=2,\dots,N-1$$

This gives N–2 equations for the determination of y" at the N dividing points. Thus two additional requirements are necessary. By using quadratic polynomals on the first and last interval y" becomes constant on these intervals, and the equation system AV–5 with the additional conditions

$$y''_1 - y''_2 = 0 \qquad \text{(AV–6)}$$

$$y''_{N-1} - y''_N = 0 \qquad \text{(AV–7)}$$

can be solved.

The linear equation set consisting of AV–6, AV–5 and AV–7 can be expressed in matrix form:

$$H_1 y'' = H_2 y \qquad \text{(AV–8)}$$

where H_1 and H_2 are tridiagonal matrices only dependent on the location of the dividing points, and y" and y are vectors of y" and y at the dividing points.

When y" has been calculated y' can be obtained from equation AV–4 which can be expressed in matrix form:

$$y' = D_1 y + D_2 y'' \qquad \text{(AV–9)}$$

Equation AV–8 and AV–9 can be rearranged to give expressions for y' and y" similar to the ones obtained by collocation techniques.

$$y' = Ay \qquad \text{(AV–10)}$$

$$y'' = By \qquad \text{(AV–11)}$$

where $B=H_1^{-1}H_2$ and $A=D_1+D_2B$ are only dependent on the location of the dividing points.

APPENDIX VI

Specifications and part list for the pilot reactor system

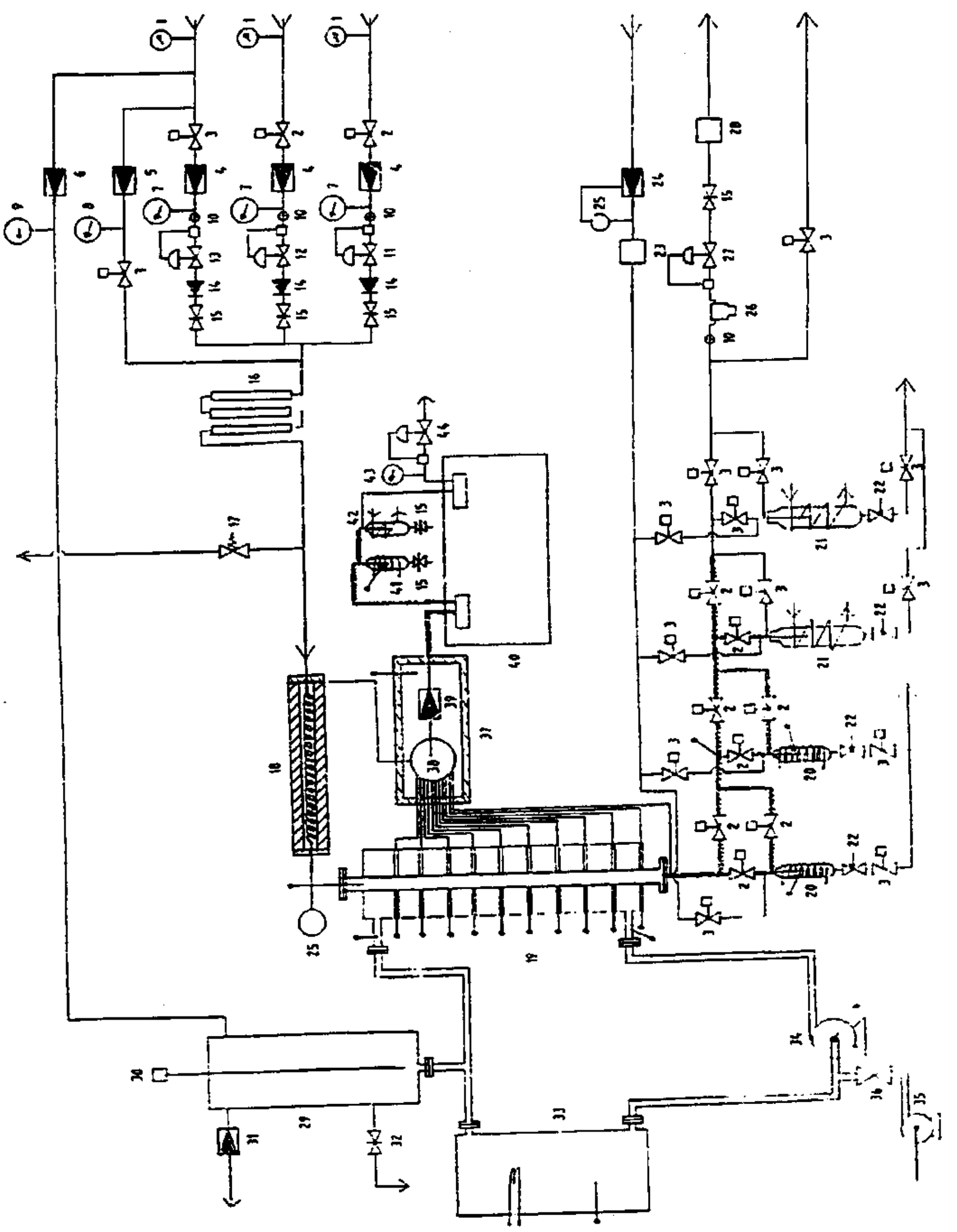

DELELISTE MED SPESIFIKASJONER

1. Manometer

Bourdon digital:	XM801 R 0–400
Ø = 100 mm	
Trykkområde:	0–400 bar
Tilkobling:	Gyrolok 4AF8–316

2. Luftdrevet magnetventil sammensatt av:

a) Kuleventil:

Kuleventil:	Hoke 7223F6Y 316SS
Max trykk:	5000 PSIG
Temperaturområde:	–29°C til +179°C
C_v–faktor:	3,4
Åpning:	0,375
Tilkobling:	Gyrolok 4CM6–316 ved inn– og utgang

b) Luftaktuator
Hoke 0219 A4 m/ hurtigkobling for 6 mm slange, type LAN618

c) Monteringsovergang
Hoke 0219 K7200

d) Grunnenhet for el–ventil
Mecman 4432

e) Spole
Mecman 220V, $50H_z$ T412/310

f) El–kontakt
Mecman 440–112

3. Luftdrevet magnetventil sammensatt av:

a) Kuleventil: Hoke 7115G4Y 316SS
Max trykk: 6000 PSIG
Temperaturområde: $-18^{0}C$ til $+149^{0}C$
C_v-faktor: 0,80
Åpning: 0,187
Tilkobling: Gyrolok 4N–316 ved inn– og utgang

b) Luftaktuator
Hoke 0219A4

c) Monteringsovergang
Hoke 0219 K7100

d) Grunnenhet for el–ventil
Mecman 4432

e) Spole
Mecman 220V, $50H_z$ T412/310

f) El–kontakt
Mecman 440–112

4. Reduksjonsventil
Tescom Pressure Regulator

Serie:	44–1100
Modell:	44–1123–24
Materiale:	316SS
Max inngangstrykk:	10 000 PSIG
Utgangstrykk:	10–1500 PSIG
Tilkobling:	Gyrolok 4CM4–316 ved inn–og utgang

5. Reduksjonsventil
   Tescom Pressure Regulator

Serie:	44–1100
Modell:	44–1112–24
Materiale:	Messing
Max inngangstrykk:	6 000 PSIG
Utgangstrykk:	0–800
Tilkobling:	Gyrolok 4CM4–316 ved inn– og utgang

6. Reduksjonsventil
   Tescom Pressure Regulator

Serie:	44–1100
Modell:	44–1121–24
Materiale:	316SS
Max inngangstrykk:	10 000 PSIG
Utgangstrykk:	0–500 PSIG
Tilkobling:	Gyrolok 4CM4–316 ved inn– og utgang

7. Manometer
   Bourdon C, MIX AISI316L. Klasse 1
   Ø = 50 mm

Trykkområde:	0–160 bar
Tilkobling:	Gyrolok 4AF4–316

8. Manometer
   Bourdon C, MIX AISI316L. Klasse 1
   Ø = 100 mm

Trykkområde:	0–160 bar
Tilkobling:	Gyrolok 4AF8–316

9. Manometer
   Bourdon digital XMS01 RO-50
   Ø = 100 mm

Trykkområde:	0-50 bar
Tilkobling:	Gyrolok 4AF8-316

10. Filter
    Hoke 6320 G4Y 316SS

Filterinnsats:	80410-3
Max trykk:	5000 PSIG
Temperaturområde:	-51°C til +232°C
C_v-faktor:	0,33
Tilkobling:	Gyrolok 4N-316 ved inn- og utgang

11. Gassregulator
    Hi-Tec Mass Flow Controller

Modell:	F122C-FA + F033C-LA (MFC)
Tilkobling:	Gyrolok 4N-316 ved inn- og utgang

Driftsdata:	
Medium:	H_2
Temperatur:	20°C
Inngangstrykk:	50 bar
Utgangstrykk:	30 bar
Max trykk:	200 bar
Kapasitet:	0,8 - 40 nl/min

12. Gassregulator
    Hi-Tec Mass Flow Controller

Modell:	F122C-FA + F033C-LA (MFC)
Tilkobling:	Gyrolok 4N-316 ved inn- og utgang

Driftsdata:

Medium:	$H_2 : CO = 2 : 1$
Temperatur:	20°C
Inngangstrykk:	50 bar
Utgangstrykk:	30 bar
Max trykk:	200 bar
Kapasitet:	1,2 – 60 nl/min

13. Gassregulator
Hi–Tec Mass Flow Controller

Modell:	F122C–FA + F033C–LA (MFC)
Tilkobling:	Gyrolok 4N–316 ved inn– og utgang

Driftsdata:

Medium:	N_2
Temperatur:	20°C
Inngangstrykk:	50 bar
Utgangstrykk:	30 bar
Max trykk:	200 bar
Kapasitet:	0,6 – 30 nl/min

14. Tilbakeslagsventil

Hoke 6133G4Y 316SS

Tilkobling:	Gyrolok 4N–316 ved inn– og utgang

15. Kuleventil

Hoke 7115G4Y 316SS

Max trykk:	6 000 PSIG
Temperaturområde:	–18°C til +149°C
C_v–faktor:	0,80
Åpning:	0,187
Tilkobling:	Gyrolok 4N–316 ved inn– og utgang

16. Rensefeller

Materiale:	1" syrefast stålrør
Lengde:	2 m
Tilkobling:	Gyrolok 16RU12–316 til Gyrolok 6R12–316 til Gyrolok 4R6–316 ved inn– og utgang

17. Sikkerhetsventil

Hoke 6548 L4Y 316SS

Max trykk:	3 000 PSIG
Trykkområde:	350–1500 PSI
Temperaturområde:	–29°C til +93°C
C_v–faktor:	1,03
Tilkobling:	Gyrolok 4CF4–316 ved inngang Gyrolok 4CM4–316 ved utgang

18. Forvarmer

Forvarmeren består av en rørspiral inne i en ovn

Rørspiral:

Materiale:	3/8" syrefast rør med veggtykkelse 0,065"
Lengde:	6 m
Tilkobling:	Gyrolok 6U–316 ved inn– og utgang

Ovn:

Ovnen er delt i to deler, hver del med lengde på 0,5 m og sammensatt av to halvsylindriske varmemoduler som er seriekoblet.

Materiale:	Fibrothal varmemoduler type HAS 200/500/110
Indre diameter:	200 mm
Ytre diameter:	350 mm
Lengde:	500 mm
Effekt:	2500 W pr. modul
Strømstyrke:	110 V pr. modul
Vekt:	4,6 kg pr. modul

Ovnskappe:

Materiale:	2 mm valset kopperplate påloddet 1/4" kopperrør til vannkjøling
Tilkobling for vannkjøling:	Gyrolok 4 U, messing

19. Reaktor med kjølekappe

Se konstruksjonstegning

20. Væskesylinder

Hoke 8HD 1000
DOT sylinder – 304SS

Max trykk:	1800 PSIG
Kapasitet:	1000 ml
Tilkobling:	Gyrolok 8TMT8–316 ved innløp Gyrolok 4CM8–316 ved utløp

21. Væskesylinder

Hoke 8HD 1G
DOT sylinder – 304SS

Max trykk:	1800 PSIG
Kapasitet:	1 gal.
Tilkobling:	Gyrolok 8TMT8–316 ved innløp
	Gyrolok 4CM8–316 ved utløp

22. Nåleventil

Milli–Mite Forged Metering valve 1300 serien

Hoke 1335 G4Y 316SS

Max trykk:	5000 PSIG
Temperaturområde:	–54°C til +232°C
C_v–faktor:	0,010
Åpning:	0,047
Tilkobling:	Gyrolok 4N–316 ved inn– og utgang

23. Gass–regulator
Hi–Tec Mass Flow Meter

Modell:	F–123C–HA–22 (MFM)
Tilkobling:	Gyrolok 4N–316 ved inn– og utgang

Driftsdata:

Medium:	N_2
Temperatur:	20°C
Inngangstrykk:	50 bar
Utgangstrykk:	30 bar
Max trykk:	200 bar
Kapasitet:	2–100 nl/min

24. Motordrevet reduksjonsventil
Tescom Motorized Actuator

Serie:	70–2000
Modell:	26–1025–24
Materiale:	316SS
Max inngangstrykk:	10 000 PSIG
Utgangstrykk:	10–1500 PSIG
Tilkobling:	Gyrolok 4CM4–316 ved inn– og utgang

25. Trykktransmitter
Jumo Piezo

Modell:	4AP–30–010
Trykkområde:	0–100 bar
Materiale:	Syrefast stål
Tilkobling:	Gyrolok 4CF8–316/RP

26. Filter
Ultra

Type:	HD 0009
Max trykk:	100 bar
Tilkobling:	Gyrolok 4CM8–316/RP ved inn– og utløp

27. Trykkregulator
Hi Tec Pressure Regulator

Modell:	P–522D–FA+F033C–LB (EPC)
Tilkobling:	Gyrolok 4N–316 ved inn– og utgang

Driftsdata:

Inngangstrykk:	30 bar
Utgangstrykk:	1 bar
Max trykk:	200 bar
Max flow:	60 nl/min

28. Gassregulator
Hi Tec Mass Flow Meter

Modell:	F–122C–HA
Tilkobling:	Gyrolok 4N–316 ved inn– og utgang

Driftsdata:	
Medium:	$H_2 : CO = 2 : 1$
Temperatur:	20°C
Inngangstrykk:	30 bar
Utgangstrykk:	1 bar
Max trykk:	200 bar
Kapasitet:	1,2 – 60 nl/min

29. Ekspansjonstank

Se konstruksjonstegning

30. Nivåmåler

Stavsonde for kontinuerlig måling
Type HR–045111

Standard elektronikkdel
Type HR–012202

Kontinuerlig nivåmålesystem
Type HR–168104

31. Reguleringsventil
Tescom Back Pressure Regulator

Serie:	44–2300
Modell:	44–2363–24
Materiale:	316SS
Trykkområde:	0–250 PSI
Max trykk:	250 PSIG
Tilkobling:	Gyrolok 4CM4–316 ved inn– og utgang

32. Kuleventil

Hoke 7115G6Y	
Max trykk:	1500 PSI
Temperaturområde:	−18°C til +179°C
C_v−faktor:	1,40
Åpning:	0,250
Tilkobling:	Gyrolok 6N−316 ved inn− og utgang

33. Oljeforvarmer
Termos

Oljeforvarmer 10 kW	
230V	
3 fase	
reg.:	2,5−7,5 kW

Termostat	
Type:	SR 5102 J 0−400C

34. Pumpe
Hermetic spalterørs motorpumpe

Type:	CNK 40/160
Væske:	Varmeolje DowthermG
Kapasitet:	250 l/min
Løftehøyde:	1 bar
Systemtrykk:	ca. 5 bar
Temperatur:	max 400°C
Materiale:	G SC−25
Motor:	3 x 220V, 50 H_z, 2770°/min, 3,0 kW

35. Pumpe
Yamada membranpumpe

Type:	DP10 − BPT
Kapasitet:	10 l/min
Tilkobling:	3/8" galvanisert rørkuplinger

36. Reguleringsventil
ARI

Modell:	STEVI P
Trykklasse:	PN25
Dimensjon:	DN65
KN-verdi:	63
Motflenser:	DN65

37. Ovn for prøvetakingsventil HVE 6T-220
220V

38. Prøvetakingsventil m/luftdreven aktuator
Valco 12-ports ventil A6CSD 12TX

Materiale:	316SS
Testtrykk:	1000 PSI
Testtemperatur:	300°C
Tilkoblinger:	Valco 1/16" nuts og ferruler
Magnetventil:	41 El/220V

39. Reduksjonsventil
Tescom Pressure Reducing Regulator

Serie:	44-4800
Modell:	44-4861-241
Materiale:	316SS
Max inngangstrykk:	3000 PSIG
Utgangstrykk:	0,07-3,45 bar
Tilkobling:	Gyrolok 4CM4-316 ved inn- og utgang

40. Gasskromatograf
    Hewlett Packard
    Type 5890
    Serie # 2436G06349

41. Væskesylinder

    Hoke 4HD300
    DOT-sylinder 304SS

Max trykk:	1800 PSIG
Kapasitet:	300 ml
Tilkobling:	Gyrolok 4TMT4-316 ved innløp
	Gyrolok 4CM4-316 ved utløp

42. Væskesylinder

    Hoke 4HD 500
    DOT-sylinder 304SS

Max trykk:	1800 PSIG
Kapasitet:	500 ml
Tilkobling:	Gyrolok 4TMT4-316 ved innløp
	Gyrolok 4CM4-316 ved utløp

43. Manometer

Bourdon C, Mix:	316SS klasse 1
Ø = 100 mm	
Trykkområde:	0-4 bar
Tilkobling:	Gyrolok 4AF8-316

44. Gass regulator
Hi Tec Mass Flow Controller

Modell:	F-201D-FA (MFC)
Tilkobling:	Gyrolok 4N-316 ved inn- og utgang

Driftsdata:	
Medium:	H_2:CO = 2:1
Temperatur:	20°C
Inngangstrykk:	2 bar
Utgangstrykk:	1 bar
Max trykk:	64 bar
Kapasitet:	1-50 n ml/min